Ann. Geophys., 28, 621–631, 2010
www.ann-geophys.net/28/621/2010/

Annales Geophysicae

Importance of including ammonium sulfate ($(NH_4)_2SO_4$) aerosols for ice cloud parameterization in GCMs

P. S. Bhattacharjee[1], **Y. C. Sud**[2], **X. Liu**[3], **G. K. Walker**[4], **R. Yang**[1], **and J. Wang**[5]

[1]Department of Geography and Geoinformation Science, George Mason University, Fairfax, VA, USA
[2]Emeritus Meteorologist, Climate and Radiation Branch, Laboratory for Atmospheres Goddard Space Flight Center, Greenbelt, MD, USA
[3]Pacific Northwest National Laboratory, Richland, WA, USA
[4]SAIC/General Sciences Operation, Beltsville, MD, USA
[5]Department of Geosciences, University of Nebraska, Lincoln, NE, USA

Received: 31 March 2009 – Revised: 16 January 2010 – Accepted: 18 January 2010 – Published: 22 February 2010

Abstract. A common deficiency of many cloud-physics parameterizations including the NASA's microphysics of clouds with aerosol-cloud interactions (hereafter called McRAS-AC) is that they simulate lesser (larger) than the observed ice cloud particle number (size). A single column model (SCM) of McRAS-AC physics of the GEOS4 Global Circulation Model (GCM) together with an adiabatic parcel model (APM) for ice-cloud nucleation (IN) of aerosols were used to systematically examine the influence of introducing ammonium sulfate $(NH_4)_2SO_4$ aerosols in McRAS-AC and its influence on the optical properties of both liquid and ice clouds. First an $(NH_4)_2SO_4$ parameterization was included in the APM to assess its effect on clouds vis-à-vis that of the other aerosols. Subsequently, several evaluation tests were conducted over the ARM Southern Great Plain (SGP) and thirteen other locations (sorted into pristine and polluted conditions) distributed over marine and continental sites with the SCM. The statistics of the simulated cloud climatology were evaluated against the available ground and satellite data. The results showed that inclusion of $(NH_4)_2SO_4$ into McRAS-AC of the SCM made a remarkable improvement in the simulated effective radius of ice cloud particulates. However, the corresponding ice-cloud optical thickness increased even more than the observed. This can be caused by lack of horizontal cloud advection not performed in the SCM. Adjusting the other tunable parameters such as precipitation efficiency can mitigate this deficiency. Inclusion of ice cloud particle splintering invoked empirically further reduced simulation biases. Overall, these changes make a substantial improvement in simulated cloud optical properties and cloud distribution particularly over the Intertropical Convergence Zone (ITCZ) in the GCM.

Keywords. Atmospheric composition and structure (Aerosols and particles; Cloud physics and chemistry) – Meteorology and atmospheric dynamics (Climatology)

Correspondence to: P. S. Bhattacharjee
(perths3@gmail.com)

1 Introduction

Scores of papers have documented a substantial increase in anthropogenic aerosol loading over Asia and its possible impact on the environment, particularly on clouds and rainfall over many regions of the world particularly in the industrially developing regions of India and East Asia through the aerosol direct (ADE) and indirect effect (AIE) (e.g., Rosenfeld, 2000; Nakajima et al., 2001; Menon, 2002; Chylek et al., 2006; Krishnamurti et al., 2009). AIE parameterizations in the present-day atmospheric general circulation models (GCM) allow aerosols to be activated as cloud condensation nuclei (CCN) for liquid clouds and ice nuclei (IN) for ice clouds. Larger number concentrations of CCN or IN generally, even though not always, produce more cloud particles that in turn can reduce the precipitation efficiency, and thereby affect the life cycle of clouds; in this way, aerosols can influence the hydrological cycle simulation in a GCM (Lohmann and Feichter, 2005). Indeed, several recent papers and cloud chamber experiments show that the nucleating properties of complex internally mixed aerosols are not well understood, particularly for mixed and ice phase clouds (Fowler et al., 1996; Jacob, 2002; Quante and Starr, 2002). Accordingly, the latest Intergovernmental Panel on Climate Change (IPCC, 2007) noted that AIE is one of the major uncertainties of the anthropogenic climate forcing. The

numerical model based estimates of the Twomey (1974) effect of AIE range from -0.22 to $-1.85\,W\,m^{-2}$ while there are several outstanding unresolved issues relating to the complexities of the Albrecht (1989) effect of aerosols. Many recent works are directed to reduce this uncertainty (e.g., McComiskey and Feingold, 2008; Storelvmo et al., 2009).

McRAS-AC (Sud and Walker, 1999a, b; Sud and Lee, 2007) is an end-to-end parameterization of cloud dynamics, and aerosols-cloud-radiation interactions in GCMs. It has been used in some recent studies with the fvGCM (e.g., Krishnamurti et al., 2009; Wilcox et al., 2009). The former study simulated an observationally supported influence of Bombay plume on winter monsoon in and around India, while the later study found a reasonable sensitivity of North and South American aerosols on the circulation and rainfall. Moreover, Sud et al. (2009) found that both direct and indirect effects of aerosols simulated similar impact over India and Africa and that their joint effect was often more than sum of their individual effects. In other words, both the direct and indirect aerosol effects work in concert to increase the optical thickness of the atmosphere, reduce the solar radiation reaching the surface, and modify the temperature profile of the atmosphere to affect moist-convection, which is the major source of the summer season precipitation. Accordingly, even though the GCM simulated aerosol climatology and circulation characteristics were different over India and Africa, the overall AIE simulated effects were similar. The research was conducted with the current model despite the biases in the IN part of the cloud optical properties, the focus of the current study.

The research reported here was motivated by the large biases in the ice clouds simulated with McRAS-AC in the fvGCM (Klein et al., 2008; Morrison et al., 2008). NASA GSFC single column model (SCM) was used to examine the aerosol-cloud interactions over several regions to isolate the causes of aforementioned biases. Clearly, these biases are closely linked to the precipitation microphysics affecting aerosol-cloud-radiation interactions whereby we can expect to significantly ameliorate, if not entirely mitigate, these biases. Talbot et al. (1998) found presence of NH_4^+ in the upper troposphere and Tabazadeh and Toon (1998) have shown that ammonium sulfate ($(NH_4)_2SO_4$) aerosols can influence the cirrus clouds. These studies showed potential impact of ammonia and ammonium sulfate on ice clouds and that motivated the present investigation. Agricultural activities, fertilizers and livestock contribute significantly to the ammonia emissions; this suggests substantial sources of ammonia over India, China, Europe, American Midwest and southern Brazil. Ammonia gas neutralizes the sulfuric acid aerosols in the atmosphere. This reaction produces ammonium sulfate aerosols (Seinfeld and Pandis, 1998). Several laboratory and modeling studies have been conducted to determine the nucleating properties of $(NH_4)_2SO_4$ on clouds, particularly for its role in ice cloud nucleation (Martin, 1998; Cziczo and Abbatt, 1999; Bertram et al., 2000; Chen et al., 2000; Prenni et al., 2001; Chelf and Martin, 2001; Hung et al., 2002; Zuberi et al., 2002). Abbatt et al. (2006)'s cloud chamber experiments have shown the potential of solid $(NH_4)_2SO_4$ for cirrus cloud formation through heterogeneous ice nucleation. Lohmann and Leck (2005) also used $(NH_4)_2SO_4$ along with other organic particles as activated nuclei in a Lagrangian parcel model to simulate ice clouds over the Arctic. Evidently, the role of $(NH_4)_2SO_4$ as IN is being reaffirmed in several recent studies; this is consistent with its potential for increasing the IN concentrations, a well-recognized deficiency of aerosol forced ice clouds (Curry et al., 1996; Lohmann et al., 2008).

Wang et al. (2008) used a chemical transport model (Harvard's GEOS-CTM) to explicitly simulate the hysteresis of $(NH_4)_2SO_4$ particles phase transitions, and found that solid $(NH_4)_2SO_4$ dominate the sulfate budget in the upper troposphere, suggesting the importance of solid $(NH_4)_2SO_4$ for addressing the ice-cloud deficiency. The archived model outputs provide solid and liquid $(NH_4)_2SO_4$ particle-mass globally from the surface to the upper troposphere. The Wang et al. (2008) dataset was used to prescribe the $(NH_4)_2SO_4$ and assess its influence on the ice clouds simulated in McRAS-AC.

2 Model and methodology

We used an SCM version of the cloud physics of Goddard Earth Observing System (Version 4) finite volume General Circulation Model (called GEOS4-fvGCM). The model's cloud physics is called the Microphysics of clouds with Relaxed Arakawa–Schubert Scheme (McRAS) (Sud and Walker, 1999a, b; Sud and Walker, 2003). Its new aerosol cloud interaction modules, called AC, employ four sub-models to provide an end-to-end parameterization for aerosol-cloud-radiation interactions as McRAS-AC. The parameterization modules comprise of: Fountoukis and Nenes scheme (2005) aerosol activation for liquid cloud particles, Seifert and Beheng (2001, 2006) precipitation microphysics modified for a coarse resolution GCM (Sud and Lee, 2007), Khvorostyanov and Curry (1999) scheme for inferring effective radius and optical properties of clouds, together with Liu and Penner (2005) parameterization for ice and mixed phase clouds drawn from Liu et al. (2007). We introduced $(NH_4)_2SO_4$ as an additional aerosol in the SCM, while all the other IN parameterizations, like H_2SO_4 for homogeneous, soot/black carbon for immersion, and dust for deposition and contact nucleation remained the same.

2.1 Aerosol activation for CCN and IN

Both aerosol-activation algorithms, one for CCN and one for IN, are based on first principles of aerosol activation physics and assume lognormal size distribution of the aerosol species in the atmosphere (Fountoukis and Nenes, 2005).

We compute number density of activated aerosols as a function of temperature, pressure, vertical velocity and hydrochemical properties of different aerosol species that are defined in turn by mass and number concentrations of all modes of each aerosol specie. In the simulations, aerosol mass and its spatial distribution were prescribed from monthly climatology of 2-year GOCART (Goddard Chemistry Aerosol Radiation and Transport) simulation (Chin et al., 2002). The $(NH_4)_2SO_4$data, available as the mass-field climatology (Wang et al., 2008), was employed to compute number concentration of $(NH_4)_2SO_4$ aerosols; it was assumed to have a modal diameter of 0.14 µm. This distribution was added to the Fountoukis and Nenes (2005) as well as Liu and Penner (2005) parameterization(s) for the liquid and ice clouds, involving homogenous and heterogeneous nucleation of ice clouds.

An adiabatic cloud parcel model (APM) was used for simulating the behavior of IN and growth of ice crystals in a cold cloud for a non-precipitating parcel of air rising adiabatically at constant vertical velocity (Liu and Penner, 2005; Lin et al., 2002). Liu and Penner (2005) employed the APM to simulate both homogeneous freezing of liquid solutions and heterogeneous nucleation on solid particle (dust deposition and soot immersion), as well as resolving the competition between different particle types and modes. The APM simulations were tested and compared by invoking $(NH_4)_2SO_4$ vis-à-vis the sulfuric acid (H_2SO_4) which is a common sulfate aerosol that activates cold cirrus clouds; naturally, this happens in conjunction with the dust (deposition nucleation) aerosols, another potent aerosol for ice cloud nucleation.

2.2 Homogenous nucleation for ice

Homogeneous nucleation refers to freezing of supercooled liquid solution cloud drop at temperature below −37 °C (Curry and Webster, 1999) to form cloud ice particles. For homogeneous nucleation, the effective freezing temperature is computed from Sassen and Dodd (1988); as a function of size and molality of the cloud solution droplet. It is given by

$$T_{\text{eff}} = T + \lambda \Delta T_{\text{m}} \tag{1}$$

where T_{eff} is effective freezing temperature, T is droplet temperature, ΔT_{m} is equilibrium melting point depression; all temperatures are expressed in degree Centigrade. The constant λ is an empirical coefficient for suppression and/or enhancement of nucleation temperature due to non-ideal interaction between condensed water and solute ions. DeMott et al. (1997) gave a polynomial expression for estimating ΔT_{m} as follows:

$$\Delta T_{\text{m}} = \Sigma c_i M^i \tag{2}$$

where M^i is molality of solution and c_i are coefficients of the polynomial with index i ranges from 1 to 4. Table 2 shows the coefficients used for H_2SO_4 and $(NH_4)_2SO_4$ in the APM. The APM used DeMott et al. (1994) expression for freezing rate of pure water by

$$J_{\text{hf}} = 10^Y \tag{3}$$

where J_{hf} (in $\text{cm}^{-3}\,\text{s}^{-1}$) is the rate at which ice germs are produced from liquid water (homogeneous freezing) and the exponent Y is approximated by Heymsfield and Milosevich (1993) expression

$$Y = -606.3952 - (52.611T_c) - (1.7439T_c^2) - (0.0265T_c^3) - (1.536 \times 10^{-4} T_c^4) \tag{4}$$

where T_c is in Centigrade. Droplet sizes and molality are inferred from the well-known Kohler equation (Kohler, 1936). Accommodation coefficient (defined as probability for a vapor molecule that hits the droplet surface to be incorporated into the bulk liquid) for water vapor condensation is taken as 0.1 for both H_2SO_4 and $(NH_4)_2SO_4$ (Leaitch et al., 1986).

2.3 Heterogeneous nucleation for ice

Heterogeneous ice nucleation takes place in presence of IN by four different mechanisms namely deposition nucleation, immersion freezing, contact freezing and condensation freezing (Curry and Webster, 1999). However, in the present study we have used deposition (for dust and solid ammonium sulfate), contact (dust) and immersion (black carbon) nucleation mechanism for the SCM simulation. Dust deposition nucleation rate is calculated using the classical theory (Pruppacher and Klett, 1997). Work on ice-germ formation from the water vapor ($\Delta F_{\text{g,S}}$) is given by

$$\Delta F_{\text{g,S}} = \frac{16\pi M_{\text{w}}^2 \sigma_{\text{i,v}}^3}{3[RT\rho_{\text{i}} \ln(S_{\text{v,i}})]^2} f(m_{i,v}, x) \tag{5}$$

where M_{w} is molecular weight of water, $\sigma_{i,v}$ is surface tension at ice-water interface, R is universal gas constant, T is temperature, ρ_{i} is density of ice, $S_{\text{v,i}}$ is saturation ratio of moist air with respect to plane ice surface, $m_{\text{i,v}}$ is the wettability parameter (cosine of contact angle with water) at the ice-vapor interface. Fletcher (1962) defined $f(m_{\text{i/v}}, x)$ as the geometric factor, a function of geometry of spherical cap and aerosol particle with radius r_{N} and critical radius r_g, with x=r_{N}/r_g (Eqs. 9–22, Pruppacher and Klett, 1997).

Nucleation rate per particle in deposition nucleation (J_{hetd}) is given by

$$J_{\text{hetd}} = \frac{4\pi^2 r_{\text{N}}^2 r_g^2 Z_{\text{S}} e}{(2\pi m_{\text{w}} kT)^{0.5}} c_{1,\text{S}} \exp[-\Delta F_{\text{g,S}}/kT] \tag{6}$$

where Z_{S} is Zeldovich factor for surface nucleation (Pruppacher and Klett, 1997), e is partial pressure of water vapor, m_{w} is mass of water molecule, $c_{1,\text{S}}$ is concentration of vapor molecules in the monolayer on the surface, k is Boltzmann's constant and S is supersaturation. APM is used to simulate clouds with air parcel starting at different initial temperatures and updraft velocities; the homogeneous and heterogeneous freezing rates (J_{hf} and J_{hetd}), are obtained by solving the above algebraic equations.

Table 1. Design of simulation experiments.

Experiment number	Model	Remarks	Figure number
1a.	Single Column Model (SCM)	Without ammonium sulfate included as CCN/IN	Figure 1
1b	Single Column Model (SCM)	With ammonium sulfate included, in the liquid phase	Not shown
2	Atmospheric Parcel Model (APM)	Homogeneous nucleation	Figure 2
3	Atmospheric Parcel Model (APM)	Homogeneous & Heterogeneous nucleation	Figure 3
4	Single Column Model (SCM)	Over 13 locations around the globe, with and without ammonium sulfate as IN	Figure 5
5	Single Column Model (SCM)	Over ARM-SGP, with ice-splintering mechanism	Figure 6

3 Simulation experiments

Several simulations, listed in Table 1, were conducted to understand and eliminate the biases in the ice clouds. The control experiment, conducted with the SCM, simulated the entire atmospheric column with liquid and ice clouds for the 3-year period of the Atmospheric Radiation Measurement (ARM) – Southern Great Plain (SGP) as a driver data provided by the ARM-SGP Working Group (Xie et al., 2004). The driver data contain lateral and surface fluxes at hourly intervals based on the analysis of observations (Zhang et al., 2001). The simulations were performed for three continuous years (1999–2001); it is the only continuous period for which the ARM-SCM data were available. The model simulations were compared with available satellite and ground observations. Ground measurements of liquid water path were taken from Microwave Radiometer Retrieval (MWRRET) (Gaustad and Turner, 2007) measurements from 1999–2005, which were then compared with MODIS total column liquid water (Collection 5) data from 2000 to 2007 (Levy et al., 2007). We also performed additional SCM simulations in which all the simulations were repeated with $(NH_4)_2SO_4$ allowed to act as a CCN, and very similar results were obtained for liquid cloud optical properties (not shown). The reason is that $(NH_4)_2SO_4$ particles are in the sub-micron size range, while most of the other liquid cloud nucleating aerosols are in micron size range; accordingly, $(NH_4)_2SO_4$ aerosols would require much higher supersaturation for activation and that does not happen as long as larger aerosols are in the mix.

The second and third experiments were performed with APM simulations; these were aimed at cloud ice particle-growth by deposition to evaluate the contribution of the $(NH_4)_2SO_4$ aerosols to the number of activated IN. In the second set of experiments, the homogeneous nucleation of $(NH_4)_2SO_4$ was compared with that of H_2SO_4 while in the third set, heterogeneous dust deposition was introduced along with homogeneous nucleation. H_2SO_4 and $(NH_4)_2SO_4$ aerosols were used in two separate simulation experiments to find the effect of dust loading when both the homogeneous and heterogeneous nucleation is allowed to produce ice cloud particles. The sulfate concentration was assumed to be $200\,cm^{-3}$ (in both cases) following Liu and Penner (2005). Wettability parameter was also kept at 0.9 in both simulations following Liu and Penner (2005). The fourth experiment was conducted over each of the thirteen locations (involving seven pristine and six polluted conditions spread over continent and ocean); these sites are based on Andreae (2009), who examined the aerosol-cloud interactions using observation data at the same locations. It includes simulations wherein the $(NH_4)_2SO_4$ was not included as an IN in the SCM, and corresponding other simulations wherein the $(NH_4)_2SO_4$ aerosols were allowed to produce IN (along with black carbon). Figure 4 shows the locations of the 13 different data-sites used to drive the corresponding SCM simulations. The locations of the stations contain seven marine and six continental sites as selected by Andreae (2009). The fifth and final simulation was conducted with ice-splintering mechanism invoked in the SCM; here we again simulated the 3-year case with the ARM-SGP driving data. $(NH_4)_2SO_4$ was also included in this simulation with the rest of the GOCART aerosols for liquid and ice activation. Forcing data for the SCM were obtained from non-constrained GCM simulations in which sea-surface temperatures (SST) were prescribed from SST analysis. The moist physics and radiation schemes were unchanged in both the GCM and SCM. Advective tendencies for temperature and specific humidity as well as surface fluxes were saved hourly at the GCM grid cell nearest to the Andeae (2009) at each selected location. We also used McRAS-AIE in fvGCM (finite volume GCM) to examine its impact on a 2 degrees latitude$\times$2.5 degrees longitude, 55 vertical levels version of the model simulations.

Table 2. Physical properties and coefficients use for nucleation of H_2SO_4 and $(NH_4)_2SO_4$ in the APM.

Physical properties	H_2SO_4 (Liu, APM)	$(NH_4)_2SO_4$ (implemented in APM)
Density	1.841 g cm^{-3}	1.77 g cm^{-3}
Molar mass	98 g mol^{-1}	132 g mol^{-1}
Surface tension formula	$118.438-0.155*(T-273.15)+$ 0.627∗molality (of H_20-H_2SO_4 solution) (after Sassen and Dodd, 1988)	$76.1-0.155*(T-273.15)$ +2.17∗molality (of H_20-$(NH_4)_2SO_4$ solution) (after DeMott, 1997)
Equilibrium melting point depression formula (ΔT_m)($T_{eff}=T+\lambda*\Delta T_m$)	ΔT_m=c1∗ms+c2∗ms^2+c3∗ms^3 +c4∗ms^4 where ms = molality c0=0.0 c1=3.513627 c2=0.471638 c3=0.033208 c4=0.02505 c5=0.0 (after Chen, 1994, and DeMott et al., 1997)	ΔT_m=c0+c1∗ms+c2∗ms^2+c3∗ms^3 +c4∗ms^4+c5∗ms^5 where ms = molality c0=0.02199 c1=4.12 c2=−1.33055 c3=0.66822 c4=−0.12445 c5=0.00832 (after Chen, 1994, and DeMott et al., 1997)
Constant for freezing to melting point depression (λ)	2.0 (after Chen et al., 2002)	1.7 (after Sassen and Dodd, 1988)

4 Results

The monthly variations of total column liquid water content (in g m^{-2}) over ARM-SGP site, as simulated by the SCM in Experiment 1, were compared with the ground-based observations and satellite data. Monthly mean and corresponding standard deviation of long-term climatology of observations data is used to plot the annual mean and standard deviations (as error bars) of liquid water path. As can be seen in Fig. 1, the climatology of liquid water path simulated by the SCM shows a realistic annual cycle that is in reasonable agreement with the ground-based remote sensing measurements and satellite data. This agreement implies a realistic annual cycle in the CCN concentrations. It also has a realistic annual cycle of cloud optical thickness and cloud drop effective radius (see Sud and Lee, 2007, for more details). However, the simulated ice clouds had much smaller ice-particle number concentration (IPNC) than observed with correspondingly lesser ice-cloud optical thickness than observed even though the total cloud ice water path was reasonable (see Fig. 5 discussed below). This deficiency is largely ameliorated by including ammonium sulfate aerosols as our simulation results show.

On the basis of the above findings, and following the foregoing discussions of the importance of $(NH_4)_2SO_4$, additional exploratory simulation experiments were conducted employing the APM, in which only the homogeneous ice nucleation were examined. Figure 2 shows the nucleating behavior of $(NH_4)_2SO_4$ compared with that of H_2SO_4 for several different vertical velocities. The IPNC per cm^{-3} at three different cloud base temperatures viz, 229.73 K, 214.2 K and 194.1 K are shown for both H_2SO_4 and $(NH_4)_2SO_4$ simulations. For comparison, we assumed lognormal size distribution with aerosol modal radius of 0.02 µm and distribution

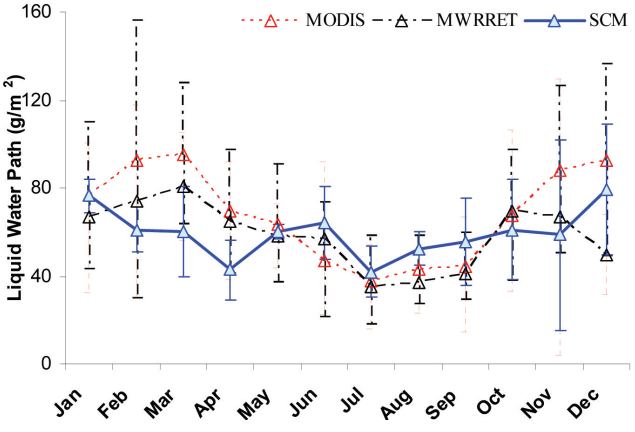

Fig. 1. Monthly average climatology of liquid water path (in g m^{-2}) over ARM-SGP by SCM (blue, solid line), MWRRET (black, dash-dot) and MODIS (red, short dashes). MWRRET measurements are between 1999–2005 and MODIS collection 5 data between March 2000 to February 2007. SCM simulation is for 3 years (1999–2001) ARM-forcing data.

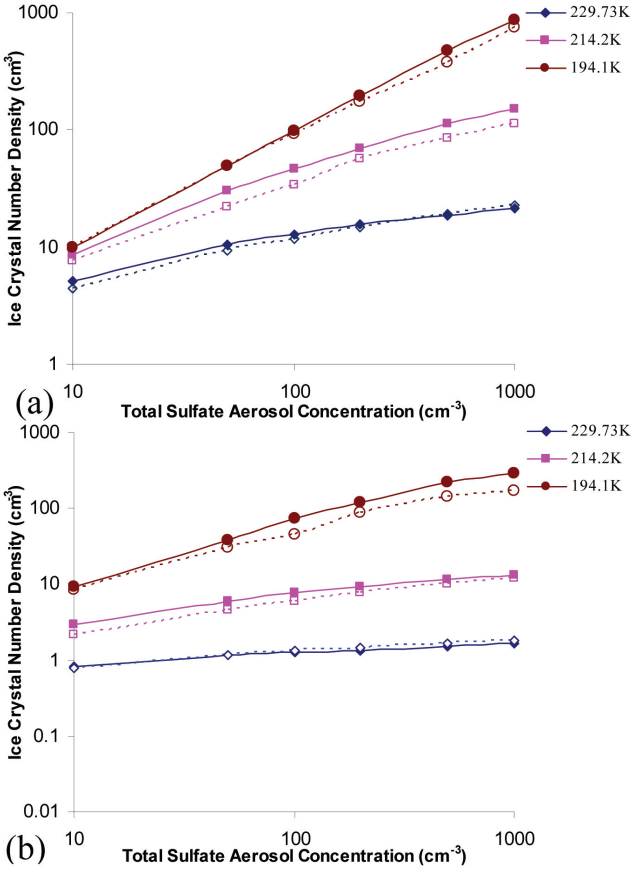

Fig. 2. APM simulation of ice crystal number density (cm^{-3}) at different cloud base temperatures (229.73 K, 214.2 K and 194.1 K) and updraft velocities of 2 m s^{-1} **(a)** and 0.5 m s^{-1} **(b)** for homogeneous freezing. $(NH_4)_2SO_4$ is represented by solid line and H_2SO_4 by dotted line.

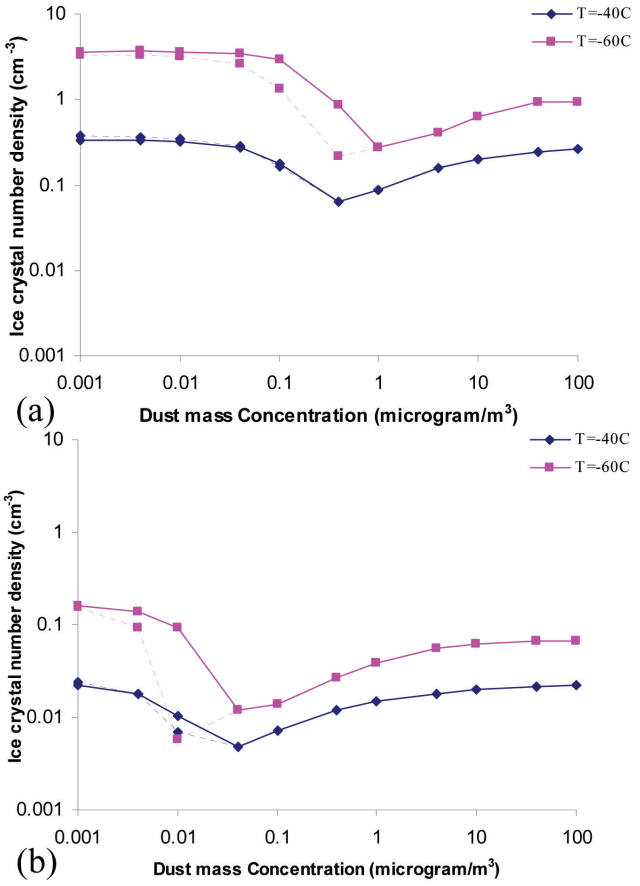

Fig. 3. APM simulation of ice crystal number density (cm^{-3}) at different dust loading for updraft velocity of 0.2 m s^{-1} **(a)** and 0.04 m s^{-1} **(b)**. Initial parcel temperatures are −40 °C and −60 °C. $(NH_4)_2SO_4$ is represented by solid line and H_2SO_4 by dotted line.

width of 2.3 for both aerosol-species (Lin et al., 2002). Initial parcel temperatures were varied from −35 °C to −80 °C, while the sulfate aerosol number concentrations varied from 10 to 1000 cm^{-3} and the updraft velocities ranged from 0.01 to 5 m s^{-1}. This gave a series of datasets that were used to infer specific values of IPNC as a function of the above three variables. The results show that effect of aerosol number concentration on IPNC is much larger when the vertical velocity is large for both species. Table 2 shows different physical parameters and coefficients used for homogeneous ice nucleation in APM for both H_2SO_4 and $(NH_4)_2SO_4$ (after Chen, 1994, and DeMott et al., 1997). Figure 2 shows similar behavior for both the H_2SO_4 and $(NH_4)_2SO_4$ at 2 m s^{-1} and 0.5 m s^{-1} updraft velocities that are consistent with Koop et al. (2000). However, $(NH_4)_2SO_4$ was found to nucleate slightly more than H_2SO_4 for lower cloud base temperatures.

In the third set of experiments both homogeneous and heterogeneous nucleation was allowed. For the dust particles a lognormal size distribution from De Rues et al. (2000) was assumed, and the mass loading was varied from 0.001 to 100 µg m^{-3}. Figure 3 shows the ice number concentration in response to dust loading when the range of vertical velocity was 0.2 and 0.04 m s^{-1} and initial parcel temperatures were varied from −40 °C to −60 °C. It is evident that homogeneous nucleation dominates when dust loading is small and it shuts off gradually with increasing dust loading. When the dust loading increases as shown on the right, heterogeneous nucleation on dust becomes more important and consumes more water vapor so the homogeneous nucleation gradually reduces and shuts off leading to decrease of IPNC. When homogeneous nucleation dominates, total IPNC is insensitive to dust aerosol number concentrations (depicted by flat curves at the left hand side of figure) since IPNC from homogeneous nucleation is much higher than that from heterogeneous nucleation. Note that with typical sulfate and dust aerosol number concentrations in the upper troposphere, ice number from pure homogeneous nucleation on sulfate (with number concentrations of a few hundreds per cm^3 in

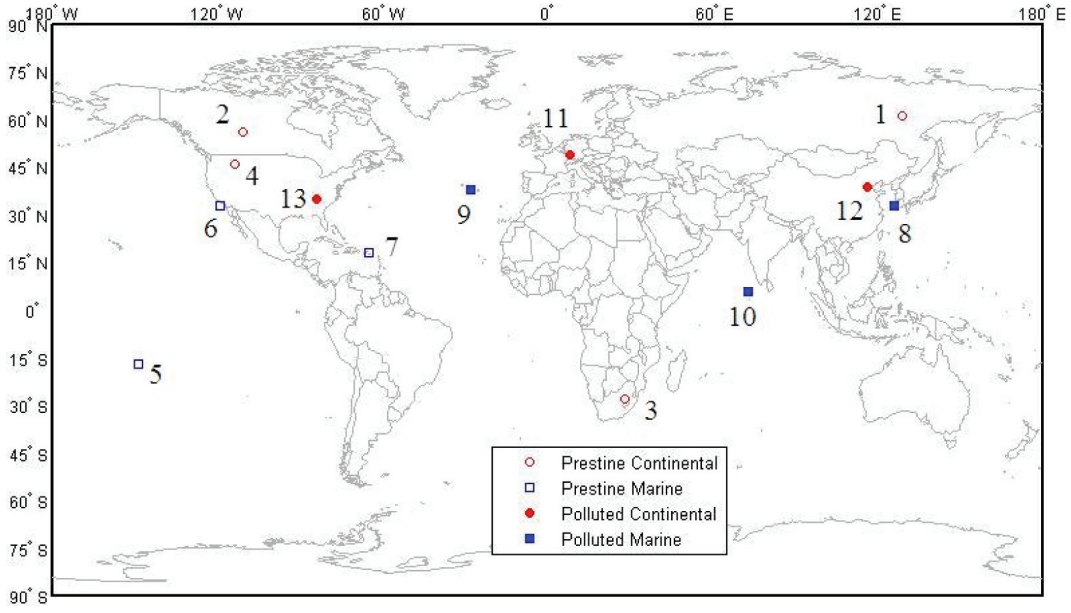

Fig. 4. Location of SCM simulation is conducted after Andreae (2009) work on polluted vs. pristine points over marine and continents. The location points correspond to the center of the markers.

Fig. 2) is much higher than that from heterogeneous nucleation on dust (with number concentrations of less than a few per cm^3 in Fig. 3). As both sulfate and dust compete to become IN in the transition zone (between the homogeneous and heterogeneous domains), heterogeneous nucleation begins to dominate while the homogenous nucleation which occurs after further cooling of a rising convective clouds is suppressed. At a colder initial temperature, but in the heterogeneous regime, $(NH_4)_2SO_4$ nucleates somewhat more than H_2SO_4 in the presence of dust nucleation.

In the fourth set of experiments, we compared the IN simulated by the SCM at several sites around the globe. In contrast to the previous experiments, in these experiments $(NH_4)_2SO_4$ aerosols were allowed to become heterogeneous IN. Figure 5 shows the simulated annual mean of vertically integrated ice-cloud optical thickness and ice particle effective radius compared with the available MODIS long-term annual mean over the same sites. MODIS annual mean is constructed from long-term monthly mean and corresponding standard deviation, which are then averaged to construct annual mean and the corresponding error bars of the data. Several major differences are notable. Figure 5 shows that the addition of $(NH_4)_2SO_4$ as an IN decreases the ice particle effective radius for all the test sites. The influence is largest over the polluted sites, particularly over land. This shows that $(NH_4)_2SO_4$ aerosols activating as IN, increased the IPNC and decreased the ice effective radius (because effective radius $r_{\text{eff}} \propto (1/N)^{1/3}$, where N is IPNC). Because the test sites are few and spread over different areas (as shown in Fig. 4), the $(NH_4)_2SO_4$ influence on the mean annual cycle of ice-nucleation behavior of aerosols was not too revealing (not shown). Nevertheless, Table 3 summarizes changes of ice optical properties in the SCM (as annual mean); it again shows the influence of $(NH_4)_2SO_4$ is most pronounced over the polluted regions particularly over land.

One of the important mechanisms of increasing IPNC is the secondary process of ice particle splintering. Ice particles are known to undergo a rimming-splintering process (Hallet and Mossop, 1974) that naturally results in an increase of IPNC with a corresponding decrease in particle size. We have used an enhancement factor of 1.2 employed by Zeng et al. (2009) for cloud particles that are created at temperatures larger than $-25\,^{\circ}$C. With this change, we conducted the fifth set of SCM simulation experiments. Figure 6a, b) shows the 3 years SCM simulations of vertical integrated ice and liquid effective radius over ARM-SGP area with splintering. Clearly introduction of $(NH_4)_2SO_4$ as an IN gave more realistic simulations with respect to the MODIS data. Monthly mean and corresponding standard deviation of long-term MODIS data (2000–2007) are used to plot the annual mean of liquid and ice particle effective radius. Splintering of cloud-ice particles increased ice-particle number concentration and decreased ice effective radius particularly in the summer months with moist convection. Small changes in liquid effective radius in this simulation are presumably due to natural variability of the model.

5 Summary and conclusions

We have conducted four different kinds of simulation experiments to examine the response of the optical properties of

Table 3. Annual mean and standard deviation of ice cloud optical properties over selected regions (Fig. 4) simulated by SCM and compared with MODIS.

Location	Ice cloud optical thickness			Ice cloud effective radius (micron)		
	Without $(NH_4)_2SO_4$	With $(NH_4)_2SO_4$	MODIS	Without $(NH_4)_2SO_4$	With $(NH_4)_2SO_4$	MODIS
Pristine, Continent	1.36 (±0.59)	20.9 (±3.83)	18.13 (±4.41	52.51 (±11.77)	31.82 (±7.52)	22.78 (±1.48)
Pristine, Marine	0.77 (±0.22)	32.62 (±1.8)	12.58 (±2.64)	53.54 (±13.16)	35.65 (±12.86)	26.02 (±2.41)
Polluted, Continent	1.36 (±0.06)	18.67 (±0.92)	15.34 ±4.57)	44.9 (±7.15)	26.42 (±8.29)	25.5 (±1.94)
Polluted, Marine	1.53 (±0.48)	19.3 (±1.63)	20.61 (±5.11)	46.05 (±3.61)	31.2 (±5.17)	23.4 (±1.83)

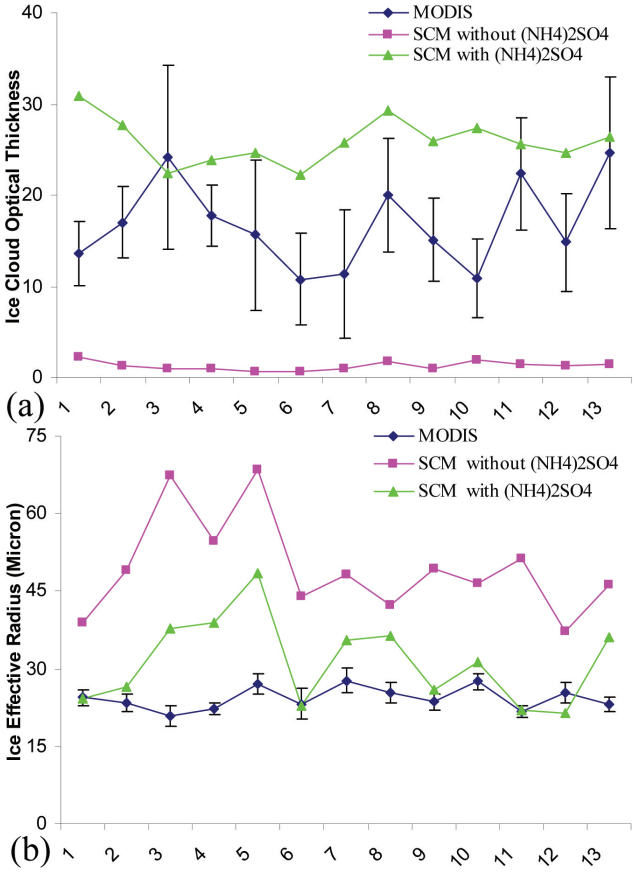

Fig. 5. SCM simulation of **(a)** ice optical thickness and **(b)** effective radius (in micron) annual mean compared against MODIS long term mean (2000–2007). Simulations are conducted with and without considering $(NH_4)_2SO_4$ as an IN in the model. X-axis is the location points in Fig. 4. Points 1–4: Pristine, Continent, 5–7: Pristine, Marine, 8–10: Polluted, Marine and 11–13: Polluted, Continent.

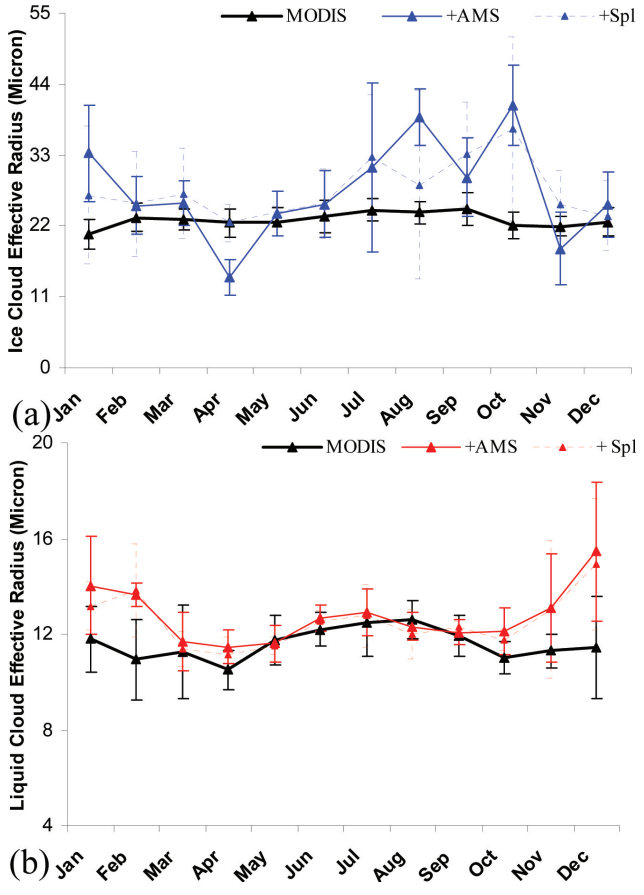

Fig. 6. SCM simulation of **(a)** ice cloud effective radius (in micron), **(b)** water cloud effective radius (in micron) over ARM-SGP site compared with MODIS long-term mean (2000–2007). X-axis is the annual mean of both model and observation data. In the figure +AMS stands for, SCM simulation with $(NH_4)_2SO_4$ and +Spl for inclusion of splintering (along with $(NH_4)_2SO_4$) in the simulation. Splintering factor is taken as 1.2 for this simulation.

both liquid and ice clouds over ARM SGP site and thirteen other locations employed by Andreae (2009). The liquid cloud mass fraction, optical properties, and cloud particle effective radius (with or without $(NH_4)_2SO_4$ acting as an IN) show reasonable agreement with observations over the ARM SGP and 13 other sites (Andreae, 2009). Nevertheless, without $(NH_4)_2SO_4$ aerosols the IPNC yield was much less than the observed particularly over the oceans. This could be caused by too small IN activation or too few IN available for activation. Literature survey indicates that it has been

a common deficiency of many models. Indeed, there many working hypotheses have been advanced to increase IN including breakup of large cloud particles by collision and turbulent wind shear.

Following the bias-reducing effects of $(NH_4)_2SO_4$ for the ice clouds in the APM evaluations, thereafter we included the $(NH_4)_2SO_4$ aerosol activation physics into the SCM and repeated the simulations. These changes had a remarkable influence on the ice particle effective radius as well as on the total IN simulated. However, simulated ice-phase optical thickness increased even more than the observed. In fact, all the selected sites consistently simulated larger optical thickness than the observed and that is "so called" overcorrection and suggests the need to retune the other disposable parameters, for example, increasing the precipitation efficiency by modifying auto-conversion and/or accretion efficiency. Alternatively, it could emanate from: i) all the $(NH4)_2SO_4$ aerosols getting activated as IN; ii) absence of cloud advection in the SCM, which, in the full GCM, allows cloud condensate to advect to adjacent grid cells thereby promoting cloud evaporation; iii) carrying too many cloud particles in the updraft of cumulus convection or not carrying the clouds high enough to let cloud particles evaporate and cloud fraction to reduce proportionally; iv) biases in the prescribed climatology of $(NH_4)_2SO_4$ aerosols over the test sites; v) absence of self-coagulation in liquid clouds; vi) shortcomings in the vertical overlapping assumption of clouds, in which three randomly overlapped superlayers contain maximally overlapped clouds (Chou and Suarez, 1994). We hope to eliminate the biases in the cloud optical thickness in our future research through systematic evaluation of the simulated cloud fields and their radiative influences. It also requires re-evaluation of the realism of cloud evaporation and addressing the assumptions affecting cloud optical thickness. This in turn can lead to even more realistic parameterization of aerosol cloud interaction for liquid, mixed phase and ice clouds. Inclusion of ice-splintering showed some scope for further improvement of the simulation compared with observation, however, one must perform sensitivity of the splintering factor and the adequate range of ice-particle splintering temperature before the entire ice-phase aerosol cloud complex is implemented into McRAS-AC.

The present work was motivated by cloud chamber experiments of Abbatt et al. (2006) that succinctly revealed the importance of $(NH_4)_2SO_4$ as a heterogeneous IN. Our APM simulations show that nucleation invoking $(NH_4)_2SO_4$ yields more ice particles; it is even greater than H_2SO_4 in the case of homogeneous nucleation. On the average there are 50–90 particles more per cm^3 for $1000\,cm^{-3}$ sulfate concentration at lower cloud base temperatures, despite using the same modal radius and standard deviation for both H_2SO_4 and $(NH_4)_2SO_4$. Inclusion of dust as heterogeneous nuclei initiates competition between homogeneous and heterogeneous deposition on the aerosol. Increase in heterogeneous IN number resulted in a decrease of IPNC of ice clouds because of the suppression of homogeneous nucleation. The threshold of dust mass concentration on the IN depends more on updraft velocity and less on the initial parcel temperature. Presence of $(NH_4)_2SO_4$ resulted in slightly higher ice number density compared to H_2SO_4. The parameterization of $(NH_4)_2SO_4$ will be developed further using the APM and subsequently incorporated in the current parameterization of ice nucleation in the SCM and GCM.

Lauer et al. (2005) and Lohmann and Hoose (2009) evaluated the influence of ammonium sulfate aerosols in the ECHAM climate model. Lohmann and Hoose (2009) have produced several improvements in ice clouds and cloud radiative forcing fields in response to the ammonium sulfate aerosols. On the other hand, our methodology is strongly anchored to fundamental nucleation processes of liquid and ice clouds as enunciated in Fountoukis and Nenes (2005), Liu and Penner (2005) and Liu et al. (2007). This became possible because McRAS (Sud and Walker, 1999a) was able to provide reasonable estimates on the cloud-scale dynamics and the associated in-cloud vertical motion fields, for both the convective and stratiform clouds that are otherwise simulated in cloud resolving models. In the end, like almost all other modelers, we also must resort to tuning/optimization of the disposable parameters to get the most realistic radiation budgets and cloud distribution in GCM applications. Clearly, we have introduced more complexity into the parameterization(s), because we believe thusly constructed algorithms have a better chance of capturing the atmospheric response to aerosol anomalies of the real world climate change scenarios involving aerosol-cloud-radiation interactions.

Acknowledgements. This work is funded by NASA grants NNX06AF30G-Global Environmental Change-hazards and regional impacts, NASA Earth and Space Science Fellowship (NESSF) grant NNX08AV02H, and NASA MAP program (NNX09AI80G). The other authors are funded through MAP proposal. The Pacific Northwest National Laboratory is operated for the DOE by Battelle Memorial Institute under contract DE-AC06-76RLO 1830. We also thank Xiping Zeng for helpful discussion on ice particle splintering and our reviewers for useful recommendations for better clarity and comparison to other GCM parameterizations.

Topical Editor F. D'Andrea thanks three anonymous referees for their help in evaluating this paper.

References

Abbatt, J. P. D., Benz, S., Cziczo, D. J., Kanji, Z., Lohmann, U., and Mohler, O.: Solid ammonium sulfate aerosols as ice nuclei: A pathway for cirrus cloud formation, Science, 313, 1770–1773, 2006.

Adams, P. J., Seinfeld, J. H., Koch, D., Mickley, L., and Jacob, D.: General circulation model assessment of direct radiative forcing by the sulfate-nitrate-ammonium-water inorganic aerosol system, J. Geophys. Res., 106(D1), 1097–1111, 2001.

Albrecht, B. A.: Aerosols, cloud microphysics, and fractional cloudiness, Science, 245, 1227–1230, 1989.

Andreae, M. O.: Correlation between cloud condensation nuclei concentration and aerosol optical thickness in remote and polluted regions, Atmos. Chem. Phys., 9, 543–556, 2009, http://www.atmos-chem-phys.net/9/543/2009/.

Bertram, A. K., Koop, T., Molina, L. T., and Molina, M. J.: Ice formation in $(NH_4)_2SO_4$-H_2O particles, J. Phys. Chem. A, 104, 584–588, 2000.

Chelf, J. H. and Martin, S. T.: Homogeneous ice nucleation in aqueous ammonium sulfate aerosol particles, J. Geophys. Res., 106, 1215–1226, 2001.

Chen, J. P.: Theory of deliquescence and modified Kohler curves, J. Atmos. Sci., 51, 3505–3516, 1994.

Chen, Y., DeMott, P. J., Kreidenweis, S. J., Rogers, D. C., and Sherman, D. E.: Ice formation by sulfate and sulfuric acid aerosol particles under upper tropospheric conditions, J. Atmos. Sci., 57, 3752–3766, 2000.

Chen, Y., Kreidenweis, S. M., McInnes, L. M., Rogers, D. C., and DeMott, P. J.: Single particles analyses of ice nucleating aerosols in the upper troposphere and lower stratosphere, Geophyscs. Res. Lett., 25, 1391–1394, 2002.

Chin, M., Ginoux, P., Kinne, S., Torres, O., Holben, B. N., Duncan, B. N., Martin, R. V., Logan, J. A., Higurashi, A., and Nakajima, T.: Tropospheric aerosol optical thickness from the GOCART model and comparisons with satellite and Sun photometer measurements, J. Atmos. Sci., 59, 461–483, 2002.

Chou, M.-D. and Suarez, M. J.: An efficient thermal infrared radiation parameterization for use in general circulation models, NASA Tech. Memo. 104606, vol. 3, 1994.

Chylek, P., Dubey, M. K., Lohmann, U., Ramanathan, V., Kaufman, Y. J., Lesins, G., Hudson, J., Altmann, G., and Olsen, S.: Aerosol indirect effect over the Indian Ocean, Geophys. Res. Lett., 33, L06806, doi:10.1029/2005GL025397, 2006.

Curry, J. A., Rossow, W. B., Randall, D. A., and Schramm, J. L.: Overview of Arctic cloud and radiation characteristics, J. Climate, 9, 1731–1764, 1996

Curry, J. A. and Webster, P. J.: Thermodynamics of the atmospheres and oceans, InT. Geophysics Series vol. 65, Academic Press San Diego, California, 1999.

Cziczo, D. J. and Abbatt, J. P. D.: Deliquescence, efflorescence and supercooling of ammonium sulfate aerosols at low temperature: Implications for cirrus cloud formation and aerosol phase in the atmosphere, J. Geophys. Res., 104, 13781–13790, 1999.

De Reus, M., Dentener, F., Thomas, A., Borrmann, S., Ström, J., and Lelieveld, J.:, Airborne observations of dust aerosol over the North Atlantic Ocean during ACE 2: Indications for heterogeneous ozone destruction, J. Geophys. Res., 105(D12), 15263–15275, 2000.

DeMott, P. J., Meyers, M. P., and Cotton, W. R.: Parameterization and impact of ice initiation processes relevant to numerical model simulations of cirrus clouds, J. Atmos. Sci., 51, 77–90, 1994.

DeMott, P. J., Rogers, D. C., and Kreidenweis, S. M.: The susceptibility of ice formation in upper tropospheric clouds to insoluble aerosol components, J. Geophys. Res., 102(D16), 19575–19584, 1997.

Fletcher, N. H.: Physics of rain clouds, Cambridge University Press, London, 1962.

Fountoukis, C. and Nenes, A.: Continued development of a cloud droplet formation parameterization for global climate models, J. Geophys. Res-Atmos., 110, D11212, doi:10.1029/2004JD005591, 2005.

Fowler, L. D., Randall, D. A., and Rutledge, S. A.: Liquid and ice cloud microphysics in the CSU general circulation model. part I: Model description and simulated microphysical processes, J. Climate, 9, 489–529, 1996.

Gaustad, K. L. and Turner, D. D.: MWRRET Value-Added Product: The Retrieval of Liquid Water Path and Precipitable Water Vapor from Microwave Radiometer (MWR) Datasets, ARM Technical Report, DOE/SC-ARM/TR-081, 2007.

Hallet, J. and Mossop, S. C.: Production of secondary ice particles during the rimming process, Nature, 249, 26–28, 1974.

Heymsfield, A. J. and Miloshevich, L. M.: Homogeneous ice nucleation and supercooled liquid water in orographic wave clouds, J. Atmos. Sci., 50, 2335–2353, 1993.

Hung, H., Malinowski, A., and Martin, S. T.: Ice nucleation kinetics of aerosols containing aqueous and solid ammonium sulfate particles, J. Phys. Chem. A, 106, 293–306, 2002.

Intergovernmental Panel on Climate Change (IPCC) Climate Change: Summary for policymakers, in Climate Change 2007: The Scientific Basis: Contribution of Working Group I to the Fourth Assessment Report of the Intergovernmental Panel on Climate Change, edited by: Solomon, S., Qin, D., Manning, M., et al., pp. 1–18, Cambridge Univ. Press, New York, 2007.

Jakob, C.: Ice clouds in numerical weather prediction models: Progress, problems, and prospects, in Cirrus, pp. 327–345, Oxford Univ. Press, New York, 2002.

Khvorostyanov, V. I. and Curry, J. A.: Toward the theory of stochastic condensation in clouds. Part II: analytical solutions of the gamma-distribution type, J. Atmos. Sci., 56, 3997–4013, 1999.

Klein, S. A., McCoy, R. B., Morrison, H., et al.: Intercomparison of model simulation of mixed phase clouds observed during the ARM mixed phase Arctic cloud experiment I. Single layer cloud, Q. J. Roy. Meteorol. Soc., 135, 979–1002, 2008.

Kohler, H.: The nucleus in and the growth of hygroscopic droplets, Trans. Farad. Soc., 32, 1152–1161, 1936.

Koop, T., Luo, B. P., Tsias, A., and Peter, T.: Water activity as the determinant for homogeneous ice nucleation in aqueous solutions, Nature, 406, 611–614, 2000.

Krishnamurti, T. N., Chakraborty, A., Martin, A., Lau, W. K., Kim, K.-M., Sud, Y., and Walker, G.: Impact of Arabian Sea pollution on the Bay of Bengal winter monsoon rains, J. Geophys. Res., 114, D06213, doi:10.1029/2008JD010679, 2009.

Lauer, A., Hendricks, J., Ackermann, I., Schell, B., Hass, H., and Metzger, S.: Simulating aerosol microphysics with the ECHAM/MADE GCM – Part I: Model description and comparison with observations, Atmos. Chem. Phys., 5, 3251–3276, 2005, http://www.atmos-chem-phys.net/5/3251/2005/.

Leaitch, J., Strapp, W., and Isaac, G. A.: Cloud droplet nucleation and cloud scavenging of aerosol sulphate in polluted atmospheres, Tellus, 38B, 328–344, 1986.

Levy, R. C., Remer, L. A., Mattoo, S., Vermote, E. F., and Kaufman, Y. J.: Second-generation operational algorithm: Retrieval of aerosol properties over land from inversion of Moderate Resolution Imaging Spectroradiometer spectral reflectance, J. Geophys. Res., 112, D13211, doi:10.1029/2006JD007811, 2007.

Lin, R.-F., Starr, D. O/C., DeMott, P., Cotton, R., Sassen, K., Jensen, E., Kärcher, B., and Liu, X.: Cirrus parcel model comparison project phase 1: The critical components to simulate cir-

rus initiation explicitly, J. Atmos. Sci., 59, 2305–2329, 2002.

Liu, X. and Penner, J. E.: Ice nucleation parameterization for global models, Meteorol. Z., 14(4), 499–514, 2005.

Liu, X., Penner, J., Ghan, S., and Wang, M.: Inclusion of ice microphysics in the NCAR Community Atmospheric Model Version 3 (CAM3), J. Climate, 20, 4526–4547, 2007.

Lohmann, U. and Feichter, J.: Global indirect aerosol effects: a review, Atmos. Chem. Phys., 5, 715–737, 2005, http://www.atmos-chem-phys.net/5/715/2005/.

Lohmann, U. and Leck, C.: Importance of submicron surface-active organic aerosols for pristine arctic clouds, Tellus B, 57(3), 261–168, 2005.

Lohmann, U., Spichtinger, P., Jess, S., Thomas, P., and Herman S.: Cirrus cloud formation and ice supersaturation regions in a global climate model, Environ. Res. Lett., 3, 040522, doi:10.1088/1748-9326/3/4/045022, 2008.

Lohmann, U. and Hoose, C.: Sensitivity studies of different aerosol indirect effects in mixed-phase clouds, Atmos. Chem. Phys., 9, 8917–8934, 2009, http://www.atmos-chem-phys.net/9/8917/2009/.

Martin, S. T.: Phase transformations of the ternary system $(NH_4)_2SO_4$-H_2SO_4-H_2O and the implications for cirrus cloud formation, Geophys. Res. Lett., 25, 1657–1660, 1998.

McComiskey, A. and Feingold, G.: Quantifying error in the radiative forcing of the first aerosol indirect effect, Geophys. Res. Lett., 35, L02810, doi:10.1029/2007GL032667, 2008.

Menon, S., Hansen, J., Nazarenko, L., and Luo, Y.: Climate effects of black carbon aerosols in China and India, Science, 297, 2250–2253, 2002.

Morrison, H., McCoy, R., Klein, S. A., et al.: Intercomparison of model simulation of mixed phase clouds observed during the ARM mixed phase Arctic cloud experiment II. Multilayer cloud, Q. J. Roy. Meteorol. Soc., 135(641), 1003–1019, 2008.

Nakajima, T., Higurachi, A., Kawamoto, K., and Penner, J. E.: A possible correlation between satellite-derived cloud and aerosol microphysical parameters, Geophys. Res. Lett., 28, 1171–1174, 2001.

Prenni, A. J., Wise, M. E., Brooks, S. D., and Tolbert, M. A.: Ice nucleation in sulfuric acid and ammonium sulfate particles, J. Geophys. Res., 106, 3037–3044, 2001.

Pruppacher, H. R. and Klett, J. D.: Microphysics of Clouds and Precipitation, Springer, New York, 1997.

Quante, M. and Starr, D. O. C.: Dynamical processes in cirrus clouds: A review of observational results, in Cirrus, pp. 346–374, Oxford Univ. Press, New York, 2002.

Rosenfeld, D.: Suppression of rain and snow by urban and industrial air pollution, Science, 287, 1793–1796, 2000.

Sassen, K. and Dodd, G. C.: Homogeneous nucleation rate for highly supercooled cirrus cloud droplets, J. Atmos. Sci., 45(8), 1357–1369, 1988.

Seifert, A. and Beheng, K. D.: A double-moment parameterization for simulating autoconversion, accretion and self collection, Atmos. Res., 59, 265–281, 2001.

Seifert, A. and Beheng, K. D.: A two-moment parameterization for mixed phase clouds. Part 1:Model description, Meteorol. Atmos. Phys., 92, 45–66, 2006.

Seinfeld, J. H. and Pandis, S. N.: Atmospheric Chemistry and Physics: From Air Pollution to Climate Change, John Wiley, Hoboken, N. J., 1998.

Storelvmo, T., Lohmann, U., and Bennartz, R.: What governs the spread in shortwave forcings in the transient IPCC AR4 models?, Geophys. Res. Lett., 36, L01806, doi:10.1029/2008GL036069, 2009.

Sud, Y. C. and Walker, G. K.: Microphysics of clouds with the relaxed Arakawa–Schubert scheme (McRAS). Part I: design and evaluation with GATE Phase III data, J. Atmos. Sci., 56, 3196–3220, 1999a.

Sud, Y. C. and Walker, G. K.: Microphysics of clouds with the relaxed Arakawa-Schubert Cumulus Scheme (McRAS). Part II: Implementation and performance in GEOS II GCM, J. Atmos. Sci., 56, 3221–3240, 1999b.

Sud, Y. C. and Walker, G. K.: New upgrades to the microphysics and thermodynamics of clouds in McRAS: SCM and GCM evaluation of simulation biases in GEOS GCM. Proceedings of the Indian National Science Academy, Part-A, Physical Sciences, 69(5), 543–565, 2003.

Sud, Y. C. and Lee, D.: Parameterization of aerosol indirect effect to complement McRAS cloud scheme and its evaluation with the 3-year ARM-SGP analyzed data for single column models, Atmos. Res., 86(2), 105–125, 2007.

Sud, Y. C., Wilcox, E., Lau, W. K.-M., Walker, G. K., Liu, X.-H., Nenes, A., Lee, D., Kim, K.-M., Zhou, Y., and Bhattacharjee, P. S.: Sensitivity of boreal-summer circulation and precipitation to atmospheric aerosols in selected regions – Part 1: Africa and India, Ann. Geophys., 27, 3989–4007, 2009, http://www.ann-geophys.net/27/3989/2009/.

Tabazadeh, A. and Toon, O. B.: The role of ammoniated aerosols in cirrus cloud nucleation, Geophys. Res. Lett., 25(9), 1379–1382, 1998.

Talbot, R., Dibb, J., and Loomis, M.: Influence of Vertical Transport on Free Tropospheric Aerosols Over the Central USA in Springtime, Geophys. Res. Lett., 25(9), 1367–1370, 1998.

Twomey, S.: Pollution and the planetary albedo, Atmos. Environ., 8, 1251–1256, 1974.

Wang, J., Hoffmann, A. A., Park, R. J., Jacob, D. J., and Martin, S. T.: Global distribution of solid and aqueous sulfate aerosols: Effect of the hysteresis of particle phase transitions, J. Geophys. Res., 113, D11206, doi:10.1029/2007JD009367, 2008.

Wilcox, E. M., Sud, Y. C., and Walker, G.: Sensitivity of boreal-summer circulation and precipitation to atmospheric aerosols in selected regions – Part 2: The Americas, Ann. Geophys., 27, 4009–4021, 2009, http://www.ann-geophys.net/27/4009/2009/.

Xie, S. C., Cederwall, R. T., and Zhang, M. H.: Developing long-term single-column model/cloud system-resolving model forcing data using numerical weather prediction products constrained by surface and top of the atmosphere observations, J. Geophys. Res-Atmos., 109, D01104, doi:10.1029/2003JD004045, 2004.

Zeng, X., Tao, W.-K., Zhang, M., Hou, A. Y., Xie, S., Lang, S., Li, X., Starr, D. O'C., and Li, X.: A contribution by ice nuclei to global warming, Q. J. Roy. Meteorol. Soc., 135, 1614–1629, 2009.

Zhang, M. H., Lin, J. L., Cederwall, R. T., Yio, J. J., and Xie, S. C.: Objective Analysis of ARM IOP Data: Method and Sensitivity, Mon. Weather Rev., 129, 295–311, 2001.

Zuberi, B., Bertram, A. K., Cassa, C. A., Molina, L. T., and Molina, M. J.: Heterogeneous nucleation of ice in $(NH_4)_2SO_4$-H_2O particles with mineral dust immersions, Geophys. Res. Lett., 29(10), 1504, doi:10.1029/2001GL014289, 2002.